

Effects of frequency-modulated pump on stimulated Brillouin scattering in inhomogeneous plasmas

Y. Chen,¹ C. Y. Zheng,^{2,3,4} Z. J. Liu,^{2,3} L. H. Cao,^{2,3,4} and C. Z. Xiao^{5,4, a)}

¹⁾*School of Electrical and Information Engineering, Anhui University of Science and Technology, Huainan, Anhui 232001, China*

²⁾*Institute of Applied Physics and Computational Mathematics, Beijing, 100094, China*

³⁾*HEDPS, Center for Applied Physics and Technology, Peking University, Beijing 100871, China*

⁴⁾*Collaborative Innovation Center of IFSA (CICIFSA), Shanghai Jiao Tong University, Shanghai 200240, China*

⁵⁾*Key Laboratory for Micro-/Nano-Optoelectronic Devices of Ministry of Education, School of Physics and Electronics, Hunan University, Changsha, 410082, China*

(Dated: 30 March 2023)

The effects of the frequency-modulated pump on stimulated Brillouin scattering (SBS) in a flowing plasma are investigated by theory analysis, three-wave simulations, one-dimensional Vlasov-Maxwell simulations, and particle-in-cell (PIC) simulations. The resonance points of SBS oscillate in a certain spatial region as time when frequency modulations are applied. There exists a certain frequency modulation that makes the velocity of resonant points close to the group velocity of seed laser, which increases the SBS reflectivity. And the SBS could be suppressed by frequency modulation with larger bandwidth. In the Vlasov-Maxwell simulations, the multi-locations autoresonance is observed in narrow bandwidth frequency modulation case, which can also increase the SBS reflectivity. Finally, one-dimensional PIC simulations confirm our conclusions and the movement of resonant points by autoresonance is consistent with our theoretical predications.

I. INTRODUCTION

Stimulated Brillouin scattering (SBS) is a common instability in inertial confinement fusion (ICF)¹⁻⁸, it contributes most of the reflectivity when the pump laser passes through the plasma region of the hohlraum⁹⁻¹³, because SBS is not sensitive to the inhomogeneity of plasma density, it can occur below n_c , where n_c is the critical density of pump laser^{14,15}. For many years, some technics about lasers are applied to mitigate parametric instabilities, such as continuous phase plates (CPPs)¹⁶, spectral dispersion (SSD)¹⁷, and laser pulses with spike trains of uneven duration and delay (STUD)¹⁸. Recently, Liu *et al.* used a multicolor alternating-polarization laser to reduce the reflectivity of SBS^{19,20}.

The broadband pump laser is a frequently-used way to suppress laser-plasma instabilities. There are two ways of making broadband lasers: multi-frequency beamlets^{21,22} and frequency modulation²³. Zhao *et al.* have used these two ways to suppress the linear growth rate of stimulated Raman scattering (SRS)^{24,25}, and in their frequency modulation model, the bandwidth needs to be larger than the growth rates of SRS. Ma *et al.* used the sunlight-like laser to nearly eliminate the growth of stimulated Raman side scattering (SRSS) in two-dimensional particle in cell (PIC) simulations²⁶. Bates *et al.* use the pump laser with 0.6% bandwidth to suppress the cross-beam energy transfer in direct-drive ICF²⁷. Recently, Wen *et al.* studied the movement of resonant points of SRS in an inhomogeneous plasma when frequency modulation of the pump laser is present²⁸. Inspired by this work, we conjecture that the frequency modulation pump will also make the movement of SBS resonant points in a flowing plasma, and the fre-

quency modulation may be an effective way to suppress the SBS reflectivity.

Flowing plasmas are commonly observed in direct-drive⁵ and shock ignition²⁹⁻³¹. The flowing velocity of plasma is supersonic at low density region, *i.e.* the flowing velocity is larger than the ion acoustic velocity. And the flowing velocity may influence the Landau damping of ion acoustic waves³². Thus, the influence of flowing velocity should be taken into consideration when investigating SBS in ICF. In this paper, we consider the frequency modulation effects on SBS in a plasma with nonuniform flowing velocity. First, we theoretically study the movement of resonant points when frequency modulation is applied, and find that the effective interaction length achieves maximum when η (define later) is close to 1, and the velocity of resonant points is close to the group velocity of the seed laser. Through three-wave simulations, we find that the SBS reflectivity also gets maximum when η is near to 1, and SBS reflectivity is reduced when $\eta > 2.3$. Then the Vlasov-Maxwell (Vlasov) code is used to study the nonlinear effects induced by frequency-modulated pump, we find that the autoresonance not only occurs in no bandwidth case^{32,33}, but also occurs in $\eta \sim 1$ case, which is called the multi-locations autoresonance. The SBS reflectivity also increases as η increases to 1, and then decreases with η , which agrees well with three-wave simulations. At last, one-dimensional particle in cell simulations are used to verify our conclusions, the SBS reflectivity in different cases agrees with Vlasov simulations, and the movement of resonant points for particle trapping is consistent with our theoretical predictions.

Our results can provide some guidance for the experiments. If one uses frequency-modulated pump lasers to suppress the instabilities in flowing plasma, the $\eta \sim 1$ type modulations should be avoided, and $\eta > 2.3$ type frequency modulations are preferable choices.

This paper is structured in the following ways. Firstly, in

^{a)}Electronic mail: xiaocz@hnu.edu.cn

Sec. II, we describe the three-wave coupling equations analysis of SBS in an flowing plasma. Secondly, Vlasov simulations and PIC simulations to verify our theoretical results are performed in Sec. III and Sec. IV. At last, the conclusion and discussion about the sinusoidal density modulation are shown in Sec. V.

II. THEORETICAL ANALYSIS: THE EFFECTS OF FREQUENCY MODULATION ON SBS

A. three-wave coupling model with pump's frequency modulation

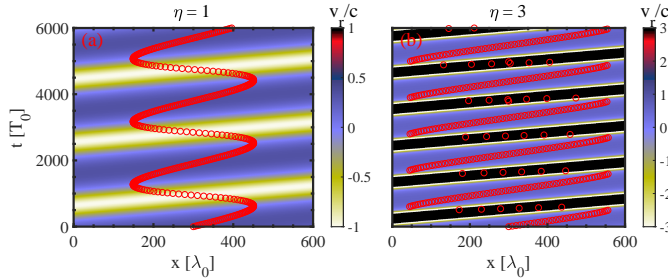


FIG. 1. Red circles are the resonant points oscillate with time and the colormap represents the velocities of resonant points. (a) The resonant points and corresponding velocity for $\eta = 1$ case. (b) The resonant points and corresponding velocity for $\eta = 3$ case.

The dominate process of SBS in ICF is back scattering, thus, one dimensional three-wave coupling model is commonly used to describe the evolution of SBS,

$$(\partial_t + V_0 \partial_x + i\delta\omega(x,t) + \nu_0)a_0 = -\frac{i}{4}\delta n_e a_1, \quad (1)$$

$$(\partial_t + V_1 \partial_x + \nu_1)a_1 = -\frac{i\omega_0}{4\omega_1}\delta n_e^* a_0, \quad (2)$$

$$(\partial_t + V_2 \partial_x + \nu_2 + iV_2\kappa'(x-x_0))\delta n_e = -\frac{i4\gamma_0^2 c^2}{\omega_0^2 v_{osc}^2} a_0 a_1^*, \quad (3)$$

where a_0, a_1 and δn_e are the envelopes of pump laser, seed laser and density perturbations of ion acoustic wave, respectively, and δn_e is already normalized to critical density n_c . ν_0, ν_1 and ν_2 are corresponding damping rates of three waves. V_0 and V_1 are the group velocity of pump laser and seed laser, $V_2 = (C_s + V(x))/c$ is the group velocity of IAW in flowing plasmas, where $C_s = \sqrt{(ZT_e + 3T_i)/m_i}$ is the ion sound speed, $V(x)$ is the flowing speed of plasmas, c is the light speed in vacuum. Z is the charge state of ions, T_e and T_i are the temperatures of electrons and ions. m_e and m_i are the mass of electrons and ions.

ω_0, ω_1 are the frequency of pump laser and seed laser, $\omega_2 = k_2(C_s + V(x))$ is the frequency of ion acoustic wave.

k_0, k_1 and k_2 are the wavenumber of three waves. $\gamma_0 = k_2 v_{osc} \omega_{pi} / 4\sqrt{\omega_0 k_2 C_s}$ is the growth rate of SBS at the resonant point, x_0 , v_{osc} is the quiver velocity of electrons in pump laser wave, $\omega_{pi} = \sqrt{Zm_e/m_i} \omega_{pe}$ ion frequency, $\omega_{pe} = \sqrt{4\pi n_e e^2 / m_e}$.

In an inhomogeneous plasma with flow, wavenumber detuning rate is obtained by

$$\kappa' \approx -\frac{1+M}{2} \frac{n_e(x_0)}{1-n_e(x_0)} \frac{k_2 C_s}{V_2 L_n} + \frac{k_2 C_s}{V_2 L_V}, \quad (4)$$

the first term in Eq. (4) comes from the plasma non-uniform, and the second term is from the plasma flow, $M = V(x)/C_s$ is the mach number, $L_n = n_e / (\partial n_e / \partial x)$ is the density scale length and $L_V = C_s / (\partial V / \partial x)$ is flow scale length. Based on early work^{34,35}, the gain of seed laser is obtained by

$$G_r = \pi \gamma_0^2 / |\kappa' V_1 V_2|. \quad (5)$$

When there is no frequency modulation of pump laser, *i.e.* $\delta\omega = 0$ in Eq. (1), the resonant point is fixed at x_0 and the interaction length is obtained from Wentzel-Kramers-Brillouin (WKB) analysis³⁴,

$$L_{int} = 2\sqrt{\frac{2\gamma_0^2}{|V_1 V_2|}}. \quad (6)$$

However, if the frequency modulation is added in pump laser, *i.e.* $\delta\omega = \omega_m \beta \sin(\omega_m t - \frac{\omega_m}{c} x)$, the resonant point will no longer be fixed, it will oscillate near x_0 , where ω_m is the modulation frequency, and $\beta = \pi/2$. By using phase match condition, $\omega_0(x,t) = \omega_1 + \omega_2(x)$, we find the equation for resonant point,

$$\omega_{00} - \omega_1 - \frac{2C_s x_r}{cL_V} + \omega_m \beta \sin(\omega_m t - \frac{\omega_m}{c} x_r) = 0, \quad (7)$$

if $\beta\omega_m \rightarrow 0$, Eq. (7) the resonant point will not move, which is same to the situation without frequency modulation.

The velocity of resonant point is obtained by applying time derivative of Eq. (7),

$$v_r = \frac{\cos(\omega_m t - \frac{\omega_m}{c} x_r)}{\frac{2\omega_0 C_s}{\beta \omega_m^2 L_V} + \cos(\omega_m t - \frac{\omega_m}{c} x_r)} c. \quad (8)$$

As we know, the velocity of seed laser equals to $-c$, the SBS gain will be increased when the velocity of resonant point is close to the velocity of seed laser, which is

$$\frac{\cos(\omega_m t - \frac{\omega_m}{c} x_r)}{\frac{2\omega_0 C_s}{\beta \omega_m^2 L_V} + \cos(\omega_m t - \frac{\omega_m}{c} x_r)} = -1, \quad (9)$$

in the time window when the velocity of resonant point is negative, $\frac{2\omega_0 C_s}{\beta \omega_m^2 L_V} = -2 \cos(\omega_m t - \frac{\omega_m}{c} x_r)$, where, $\omega_m t - \frac{\omega_m}{c} x_r = n\pi$. thus, the maximum SBS gain is achieved when

$$\frac{\omega_{00}}{\beta \omega_m^2} = \frac{L_V}{C_s}. \quad (10)$$

Here we define an indicator η to quantify the SBS gain affected by pump's frequency modulation,

$$\eta = \frac{\beta \omega_m^2 L_V}{\omega_{00} C_s}, \quad (11)$$

when $\eta = 1$, the SBS gain becomes maximum. In the small bandwidth limit with $\eta \leq 1$, the effective interaction length increases with frequency bandwidth,

$$L_{eff} = L_{int} + \alpha \Delta \omega L_V, \quad (12)$$

where $\Delta \omega = 2\beta \omega_m$, α is a constant related to the plasma parameters. As shown in Fig. 1(a), when $\eta = 1$, the red circles show the resonant points in space and time, and the color map shows the velocity of resonant points, which is obtained by Eq. (8), in the negative velocity time window, the maximum velocity of resonant points equal to $-c$, which is favor to the growth of SBS. However, when $\eta > 1$, *i.e.* frequency modulation is large, the negative velocity time window becomes short, the growth of SBS will be suppressed, as shown in Fig. 1(b), when $\eta = 3$, the negative velocity time window is much shorter than Fig. 1(a). Next, we will prove our predictions by numerically solve Eq. (1)-(3).

B. numerical results of three-wave coupling model

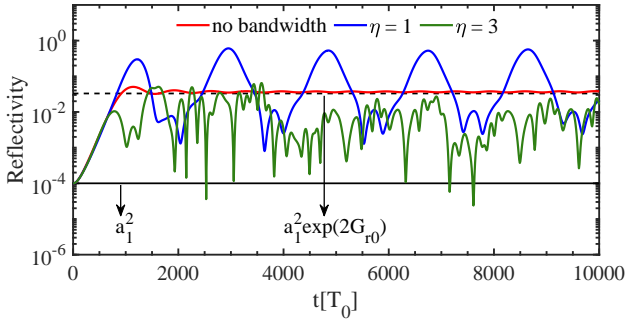


FIG. 2. Three-wave simulation results. The red line is the time dependence of SBS reflectivity with ordinary pump laser. The red line is the time dependence of SBS reflectivity for $\eta = 1$ case. The green line is the time dependence of SBS reflectivity for $\eta = 3$ case. The black dashed line is obtained by the Rosenbluth theory.

In a flowing inhomogeneous plasma, the flowing velocity and plasma density should fulfil the mass conservation law, $\partial(n_e V)/\partial x = 0$. Let us assume a linear flowing velocity in low density plasma, $V(x) = C_s(7/4 - 3x/2x_{end})$, where $x_{end} = 600\lambda_0$ is the length of simulation box, $\lambda_0 = 351\text{nm}$ is the wavelength of pump laser. If we choose the resonant density $n_{e0} = 0.1n_c$, the plasma density profile can be deduced by mass conservation law, $n_e(x) = n_{e0}C_s/V(x)$. It should be noted that the resonant plasma density locates at the center of the simulation box, and the flowing velocity of plasma at that point is equals to $-C_s$. The wavelength of seed laser is

equal to 351nm because of the zero frequency of IAW at resonant point x_0 . The intensities of pump laser and seed laser are $3 \times 10^{15}\text{W/cm}^2$ and $3 \times 10^{11}\text{W/cm}^2$, respectively.

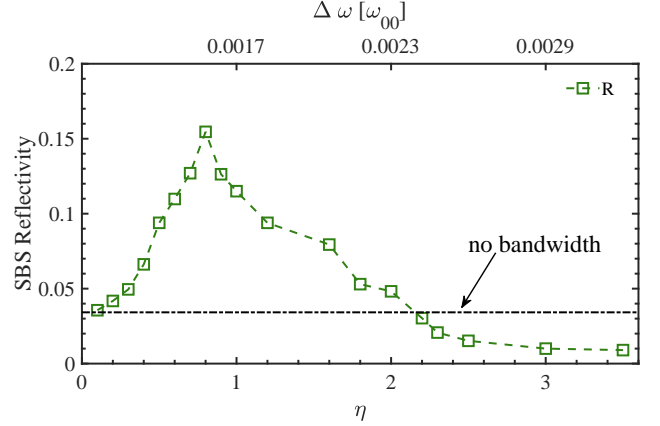


FIG. 3. Three-wave simulation results. The green squares are the average SBS reflectivity for different frequency modulations. The black dashed line represents the average reflectivity without frequency modulation. The top axis is the corresponding bandwidth of pump laser for each η .

Eq. (1)-(3) are solved by Van Leer scheme(VL3), and the damping of three waves are neglected for simplicity. We consider three different cases: (1) without frequency modulation, (2) frequency modulation with $\eta = 1$, (3) frequency modulation with $\eta = 3$. As shown in Fig. 2, the red line represents the time-dependence of SBS reflectivity without pump's frequency modulation, the average reflectivity is 3.42%, which agrees with the reflectivity obtained by Eq. (5) showed by black dashed line. Blue line is the SBS reflectivity with pump's frequency modulation for $\eta = 1$, five bumps of reflectivity are observed, and the average reflectivity is 11.5%. These bumps come from the time window of negative velocity of resonant points, because the effective interaction length are much larger at negative velocity time window than that in positive velocity time window. The green line in Fig. 2 indicates that the SBS reflectivity is significantly reduced when $\eta = 3$, which is even below the reflectivity without bandwidth case, and the average reflectivity of green line is 1%. The reason is that the effective interaction length decreases with bandwidth when $\eta \geq 1$. As shown in Fig. 3, the SBS reflectivity first increase when $0 \leq \eta \leq 0.8$ and then decreases when $\eta \geq 0.8$, which is agreed with the theoretical predictions above. We also observe that the average reflectivity is lower than that of no bandwidth case when $\eta \geq 2.3$, because when the bandwidth of pump laser is larger, the velocities of resonant points are much larger than the velocity of seed laser and the effective interaction length will be less than L_{int} .

The results of three-wave simulations show that in a flowing inhomogeneous plasma, the reflectivity of SBS is significantly increased when $\eta \approx 1$ type frequency modulation is added to pump laser, and the reflectivity is reduced by larger-bandwidth pump with $\eta > 2.3$. Thus, in experiments, one should avoid the pump laser with $\eta \approx 1$ type frequency modulations, and

choose the frequency-modulated pump laser with larger bandwidth to suppress SBS.

The evolution of SBS will enter into nonlinear region because of large amplitude of ion acoustic waves when the intensity of pump laser is high enough. The three-wave simulations did not consider the nonlinear effects of ion acoustic wave, such as nonlinear Landau damping, particle trapping and nonlinear frequency shift. In next section, we will use one-dimensional fully kinetic Vlasov-Maxwell simulations to consider the effects of frequency modulation of pump laser in nonlinear region.

III. NONLINEAR EFFECTS INDUCED BY FREQUENCY MODULATION OF PUMP LASER

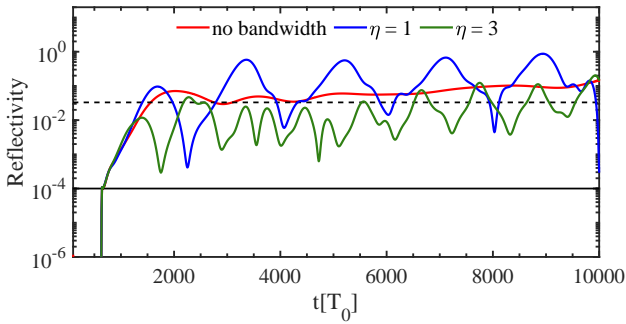


FIG. 4. Vlama simulation results. The red line is the time dependence of SBS reflectivity with ordinary pump laser. The red line is the time dependence of SBS reflectivity for $\eta = 1$ case. The green line is the time dependence of SBS reflectivity for $\eta = 3$ case. The black dashed line is obtained by the Rosenbluth theory.

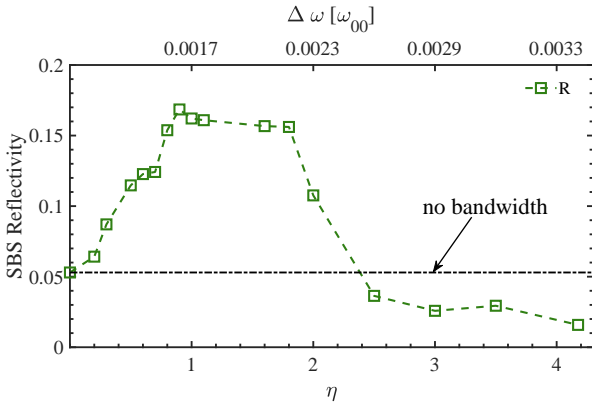


FIG. 5. Vlama simulation results. The green squares are the average SBS reflectivity for different frequency modulations. The black dashed line represents the average reflectivity without frequency modulation. The top axis is the corresponding bandwidth of pump laser for each η .

In one-dimensional Vlasov-Maxwell (Vlama) simulations, the Helium plasma is used, $Z = 2$ and $m_i = 7344m_e$, and

the temperature of electron and ion are $T_e = 1.5keV$ and $T_i = 0.5keV$, respectively. The ion acoustic velocity is obtained $C_s = 0.001152c$. The simulation box is $L = 600\lambda_0$, 10% vacuum space is reserved in the both sides and we choose the center point x_0 to be the resonant point of SBS. The flowing velocity of plasma and plasma density are the same to that in three-wave simulations. The discrete spatial unit and temporal unit are $dx = 0.31416c/\omega_{00}$ and $dt = 0.31416\omega_{00}^{-1}$, respectively. The velocity spaces of electrons and ions in simulations are $[-0.8c, 0.8c]$ and $[-0.01c, 0.01c]$. The mesh grids of distribution functions of electrons and ions in the space-velocity plane are 12000×2049 .

The wavelenghtes of unmodulated pump laser and seed laser are both 351nm, the intensities of pump laser and seed laser are same to that in three-wave simulations. The pump laser is add a frequency modulation, $E_y(t) = a_0 \cos[\omega_{00}t + \beta \sin(\omega_m t)]$, the bandwidth of pump laser is obtained by $\Delta\omega = 2\beta\omega_m$. Based on the theoretical analysis in Sec II, when $\eta = 1$, $\Delta\omega = 1.7 \times 10^{-3}\omega_{00}$, which is less than the bandwidth used in experiment $\Delta\omega = 3.0 \times 10^{-3}\omega_{00}$ ³⁶. Thus, $\eta = 1$ is possible to achieve in current experiments, however the increase of SBS reflectivity by $\eta = 1$ type bandwidth laser has not been paid enough attention.

As shown in Fig. 4, red line represents the time dependence of SBS reflectivity without frequency modulation by Vlama simulation, at early stage, $t < 4000T_0$, the evolution of SBS is in the linear stage, which is agree with Rosenbluth theory (black dashed line), however, at $t > 4000T_0$, the reflectivity becomes larger than black dashed line, because when the amplitude of ion acoustic wave increases, the frequency of ion acoustic wave decreases for the particle trapping effect, which will cancel with the detuning of non-uniform flowing velocity, the resonant point will move slowly to higher plasma density, this phenomenon is called autoresonance of SBS. The Eq. (3) in nonlinear region will change to

$$(\partial_t + V_2 \partial_x + v_2 + iV_2 \kappa'(x - x_0) + i\delta\omega_i) \delta n_e = -\frac{-i4\gamma_0^2 c^2}{\omega_{00}^2 v_{osc}^2} a_0 a_1^*, \quad (13)$$

where $\delta\omega_i$ is the nonlinear frequency shift because of particle trapping³²,

$$\frac{\delta\omega_i}{\omega_{20}} = -\zeta |\delta n_e / n_e|^{1/2}, \quad (14)$$

$\omega_{20} = k_2 C_s$ and ζ is the nonlinear frequency shift parameter defined as,

$$\zeta = \frac{1}{\sqrt{2\pi}} [\alpha_i \sqrt{\frac{ZT_e}{T_i}} (v^4 - v^2) e^{-v^2/2} - \alpha_e], \quad (15)$$

where, $\alpha_i = 0.823$ is obtained by using sudden approximation for ions, and $\alpha_e = 0.544$ is obtained by using adiabatic approximation for electrons, $v = (v_\phi - V(x))/v_{thi}$, v_ϕ is the phase velocity of ion acoustic waves and v_{thi} is the thermal velocity of ions.

In Fig. 6 (a), the ion trapping is observed at near x_0 , the frequency will shift because of the formation of vortexes. The particle trapping happens when the amplitude of ion acoustic

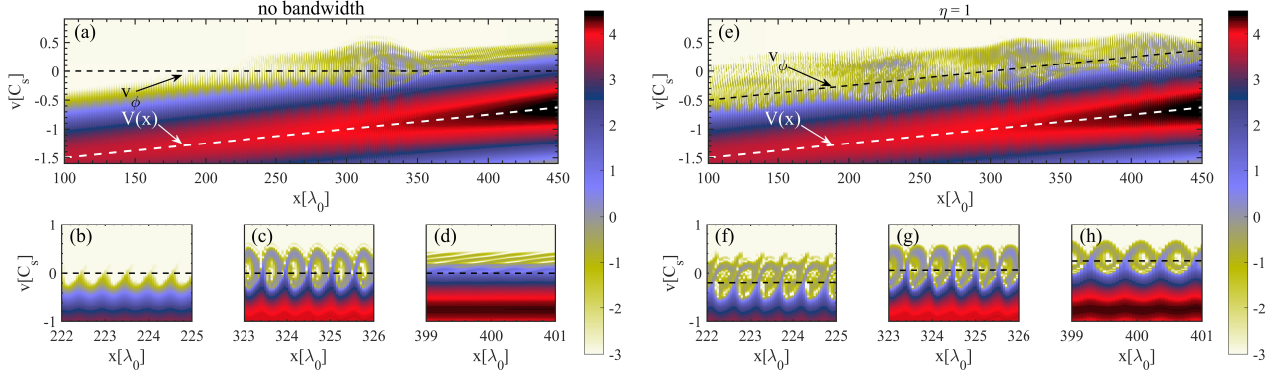


FIG. 6. Vloma simulation results. (a), (b), (c) and (d) are the particle trapping of ions in no bandwidth case. (e), (f), (g) and (h) are the particle trapping of ions in $\eta = 1$ case. Black dashed line represent the phase velocity of ion acoustic wave, and the white dashed line is the plasma flowing velocity.

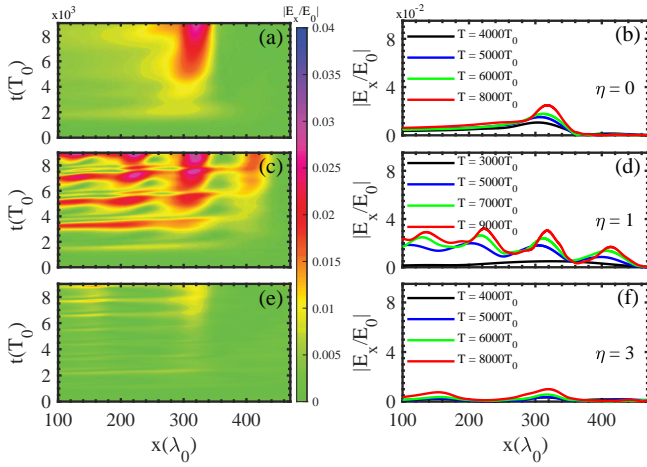


FIG. 7. (a) and (b) are the electrostatic amplitude evolution with time for no bandwidth case. (c) and (d) are the electrostatic amplitude evolution with time for $\eta = 1$ case. (e) and (f) are the electrostatic amplitude evolution with time for $\eta = 3$ case.

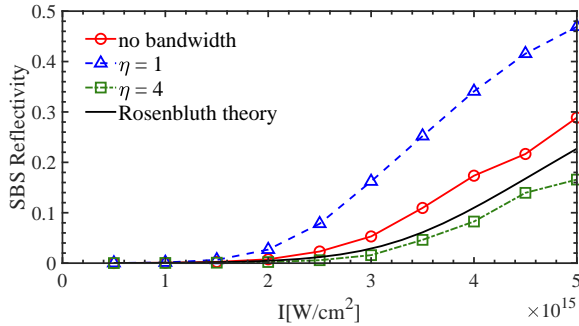


FIG. 8. The change of SBS reflectivity for different pump intensities. Red circles are the reflectivity for no bandwidth case. Blue triangles are the reflectivity for $\eta = 1$ case. Green squares are the reflectivity for $\eta = 4$ case. The black line is obtained by using Eq. (16).

wave is large, in Fig. 7(a) and (b), we can clearly observe that the peak of electrostatic field of ion acoustic wave locates at near x_0 and moves towards to higher density in nonlinear region, which is the evidence of autoresonance. We observe that the phase velocity of ion acoustic wave in Fig. 6 (b), (c) and (d) are all equal to 0, which agrees earlier work³², this may be the consequence of the resonant excitation of pump laser and seed laser.

The autoresonance is also found in $\eta = 1$ case, as shown the blue line in Fig. 4, there are five bumps similar to that in Fig. 2, but the maximum points of bumps increases as time because of autoresonance. In Fig. 6 (e), the ion trapping at four different locations are observed. Because of the $\eta = 1$ type frequency modulation, the phase velocity of ion acoustic can be consider as a linear function of x , $V_2 = V(x) + C_s$, which is agreed with the dispersion relation of ion acoustic wave in flowing plasma. Correspondingly, the auto-resonantly growth of electrostatic field in Fig. 7(c) and (d), there are four auto-resonant points, which is different from no bandwidth case. Let us explain this phenomenon, when we add $\eta = 1$ type pump laser, the effective interaction length of SBS will increase, as shown in Fig. 7(c), the interaction length in the negative velocity time window is about $300\lambda_0$, the seed laser will be amplified when it passes through interaction region, the amplified seed laser will influence the SBS at lower plasma density, the ion acoustic wave at lower density will grow rapidly as shown in Fig. 7(d). In another word, the frequency of seed does not change in the interaction region, and the change of phase velocity of ion acoustic wave results from the frequency modulation of pump laser. At lower density, the autoresonance also occurs when the frequency shift $\delta\omega_i$ cancels the wavenumber detuning term $iV_2\kappa'(x-x_0)$. This kind of multi-locations autoresonance is first observed in this paper, which will also increase the reflectivity of SBS.

The green line in Fig. 4 shows the SBS reflectivity in $\eta = 3$ case, SBS is well suppressed at linear stage, $t < 6000T_0$ because the reduction of effective interaction length, similar to the three-wave simulations in Fig. 2. However, at the nonlinear stage $t > 6000T_0$, the autoresonance also happens, and the

sbs reflectivity is larger than the Rosenbluth reflectivity (black dashed line). The autoresonance of SBS can also be observed in Fig. 7(e) and (f). The average SBS reflectivity for different η are shown in Fig. 5, the average SBS reflectivity achieves maximum at $\eta = 0.9$, and then decreases with η . The average reflectivity is lower than no bandwidth case when $\eta > 2.3$, which agrees well with our three-wave simulations in Fig. 3.

In order to investigate the influence of frequency modulation on SBS with different intensities of pump laser, we change the intensity of pump laser from $5 \times 10^{14} W/cm^2$ to $5 \times 10^{15} W/cm^2$. As shown in Fig. 8, the black line represents the theoretical reflectivity by Rosenbluth theory with considering pump depletion³⁷,

$$R = \frac{be^{(1-R)G_{r0}}}{1+b-R}, \quad (16)$$

where, $b = I_{seed0}/I_{pump}$ is the seed level, R is the SBS reflectivity. The red circles in Fig. 8 is the average SBS reflectivity without pump frequency modulation, it is larger than Rosenbluth theory (black line) when $I > 1.5 \times 10^{15} W/cm^2$, because the autoresonance of SBS happens when the pump intensity is high enough to induce particle trapping. The blue triangles are the reflectivity of $\eta = 1$ cases, which is much larger than that of no bandwidth cases (red circles). Both longer effective interaction length and multi-locations autoresonance contribute to the high level reflectivity. The reflectivity of $\eta = 4$ cases are shown by green squares, we can observe that SBS is suppressed by the large-bandwidth frequency modulation, and the reflectivity is even less than the theoretical reflectivity (black line).

In conclusion, $\eta \approx 1$ type frequency modulation of pump laser not only increase the effective interaction length but also lead to multi-locations autoresonance, the reflectivity is substantially increased. However, the large-bandwidth frequency modulation will reduce the effective interaction length and make it difficult for autoresonance to grow. Thus, large-bandwidth frequency modulation is a effective way to reduced the reflectivity of SBS.

IV. ONE-DIMENSIONAL PIC SIMULATIONS

To verify the effects of frequency-modulated pump laser on SBS, we decide to use the one-dimensional PIC code EPOCH. The plasma parameters are same as the Vlasov simulations, and we consider no bandwidth case, $\eta = 1$ case, and $\eta = 3$ case. There are 30 cells for each wavelength of pump laser and 10^4 particles in each cell for electrons and ions. We use large number of particles to reduce the thermal noise in PIC simulations. The intensity of pump laser is $3 \times 10^{15} W/cm^2$, and the seed level is $I_{seed0}/I_{pump} = 10^{-4}$. We note that the flowing velocity of plasma is set by the drifting velocity in PIC. 10% vacuum space is reserved on both sides of the simulation box, and an open boundary condition is used for both waves and particles.

As shown in Fig. 9, the red line is the reflectivity in no bandwidth case, it is larger than the Rosenbluth theory because of the autoresonance of SBS. When the $\eta = 1$ type frequency

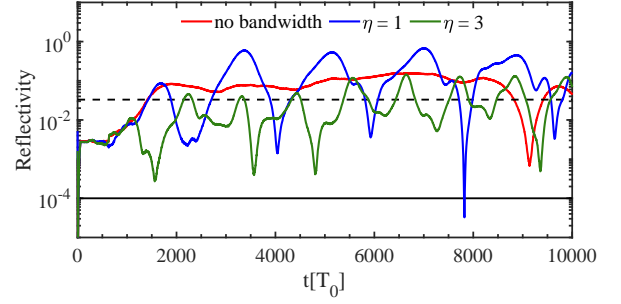


FIG. 9. PIC simulation results. The red line is the time dependence of SBS reflectivity with ordinary pump laser. The red line is the time dependence of SBS reflectivity for $\eta = 1$ case. The green line is the time dependence of SBS reflectivity for $\eta = 3$ case. The black dashed line is obtained by the Rosenbluth theory.

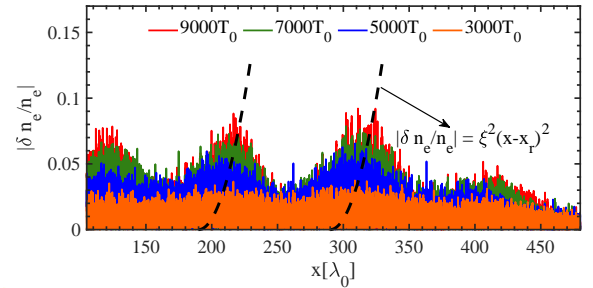


FIG. 10. PIC simulation results. The electron density perturbation at different times. We can observe four density peaks because of the autoresonance. The black dashed line is obtained by using Eq. (17).

modulation is added in pump laser, there are also five bumps of reflectivity are observed, which agree with Vlasov simulations in Fig. 9. When $\eta = 3$, the SBS is suppressed below the Rosenbluth reflectivity at early stage, however the reflectivity increases because of the autoresonance. The results of PIC simulations agree with Vlana simulation results.

We also investigate the multi-locations autoresonance in $\eta = 1$ case, the v in Eq. (15) is a constant Cs/v_{thi} in the interaction region, thus, the frequency shift parameter ζ is also a constant. As discussed in early work, when the frequency shift cancels the wavenumber detuning, the resonant points moves by obeying³²,

$$|\delta n_e / n_e| = \xi^2 (x - x_r)^2 = (V_2 k' / \zeta k_2 C_s)^2 (x - x_r)^2, \quad (17)$$

As shown in Fig. 10, the density perturbation $|\delta n_e / n_e|$ growth as time at $120\lambda_0$, $200\lambda_0$, $300\lambda_0$ and $400\lambda_0$. If there are autoresonance at these location, the resonant points will move as time. The black dashed lines are plotted by using Eq. (17), and we observe that the move of resonant points agree with theoretical predication. Thus, We have demonstrated that autoresonance occurs at these locations because of the $\eta = 1$ type frequency modulation.

V. CONCLUSION AND DISCUSSION

In this paper, first we construct a three-wave model to study the influence of frequency-modulated pump laser on SBS. We find that the reflectivity of SBS increases when η is close to 1, and the SBS will be suppressed when $\eta > 2.3$. Then, the Vlma simulations are used to investigate the nonlinear effects induced by frequency modulations, we observe the nuti-locations autoresonance when $\eta = 1$ type frequency modulation is applied. And the larger bandwidth modulation can also suppress the growth of SBS at nonlinear region. At last, the PIC simulations are used to prove our theoretical predications, and we prove that the growth of density perturbation are indeed induced by autoresonance, the move of resonant points agrees with theoretical predications.

In ICF experiments, pump laser with bandwidth is often used to mitigate the laser plasma instabilities. Early works show that the large bandwidth pump laser can restrain the growth of instabilities in homogeneous plasma. However, in a flowing inhomogeneous plasma, our results show that $\eta \approx 1$ type frequency modulation should be avoided, because it will increase the effective interaction length and even induce the nuti-locations autoresonance. We believe that the larger bandwidth modulation is a promising way to reduce the reflectivity of SBS in experiments.

ACKNOWLEDGEMENTS

We are pleased to acknowledge useful discussions with Q. Wang, Y. Z. Zhou, Y. G. Chen, N. Peng, S. Tan and W. B. Yao. This work was supported by the Strategic Priority Research Program of Chinese Academy of Sciences (Grant No.XDA25050700), National Natural Science Foundation of China (Grant Nos.11805062, 11875091 and 11975059), Science Challenge Project, No.TZ2016005 and Natural Science Foundation of Hunan Province, China (Grant No.2020JJ5029).

- ¹R. Betti, C. D. Zhou, K. S. Anderson, L. J. Perkins, W. Theobald, and A. A. Solodov, Phys. Rev. Lett. **98**, 155001 (2007).(doi: [10.1103/PhysRevLett.98.155001](https://doi.org/10.1103/PhysRevLett.98.155001))
- ²V. Tikhonchuk, Y. J. Gu, O. Klimo, J. Limpouch, and S. Weber, Matter Radiat. Extremes **4**, 045402 (2019).(doi: [10.1063/1.5090965](https://doi.org/10.1063/1.5090965))
- ³Basov N. G., Guskov S. Y. and Feokistov L. P., J. Russ. Laser Res. **13**, 396 (1992).(doi: [10.1007/BF01124892](https://doi.org/10.1007/BF01124892))
- ⁴Max Tabak, James Hammer, Michael E. Glinsky, William L. Kruer, Scott C. Wilks, John Woodworth, E. Michael Campbell, and Michael D. Perry, Phys. Plasmas **1**, 1626 (1994).(doi: [10.1063/1.870664](https://doi.org/10.1063/1.870664))
- ⁵S. E. Bodner, D. G. Colombant, J. H. Gardner, R. H. Lehmburg, S. P. Obenschain, L. Phillips, A. J. Schmitt, J. D. Sethian, R. L. McCrory, W. Seka, C. P. Verdon, J. P. Knauer, B. B. Afeyan, and H. T. Powell, Phys. Plasmas **5**, 1901 (1998).(doi: [10.1063/1.872861](https://doi.org/10.1063/1.872861))
- ⁶J. Lindl, Phys. Plasmas **2**, 3933 (1995).(doi: [10.1063/1.871025](https://doi.org/10.1063/1.871025))
- ⁷X. T. He, J.W. Li, Z. F. Fan, L. F.Wang, J. Liu, K. Lan, J. F.Wu, and W. H. Ye, Phys. Plasmas **23**, 082706 (2016).(doi: [10.1063/1.4960973](https://doi.org/10.1063/1.4960973))
- ⁸X. Ribeyre, G. Schurtz, M. Lafon, S. Galera, and S. Weber, Plasma Phys. Control. Fusion **51**, 015013 (2009).(doi: [10.1088/0741-3335/51/1/015013](https://doi.org/10.1088/0741-3335/51/1/015013))
- ⁹H. A. Rose and D. F. DuBois, Phys. Rev. Lett. **72**, 2883 (1994).(doi: [10.1103/PhysRevLett.72.2883](https://doi.org/10.1103/PhysRevLett.72.2883))
- ¹⁰P. Neumayer, R. L. Berger, L. Divol, D. H. Froula, R. A. London, B. J. MacGowan, N. B. Meezan, J. S. Ross, C. Sorce, L. J. Suter, and S. H. Glenzer, Phys. Rev. Lett. **100**, 105001 (2008).(doi: [10.1103/PhysRevLett.100.105001](https://doi.org/10.1103/PhysRevLett.100.105001))
- ¹¹J. Li, S. Zhang, C. M. Krauland, H. Wen, F. N. Beg, C. Ren, and M. S. Wei, Phys. Rev. E **101**, 033206 (2020).(doi: [10.1103/PhysRevE.101.033206](https://doi.org/10.1103/PhysRevE.101.033206))
- ¹²S. Zhang, J. Li, C. M. Krauland, F. N. Beg, S. Muller, W. Theobald, J. Palastro, T. Filkins, D. Turnbull, D. Haberberger, C. Ren, R. Betti, C. Stoeckl, E. M. Campbell, J. Trela, D. Batani, R. H. H. Scott, and M. S. Wei, Phys. Rev. E **103**, 063208 (2021).(doi: [10.1103/PhysRevE.103.063208](https://doi.org/10.1103/PhysRevE.103.063208))
- ¹³C. Z. Xiao, Y. G. Chen, J. F. Myatt, Q. Wang, Y. Chen, Z. J. Liu, C. Y. Zheng, and X. T. He, Phys. Rev. E **104**, 065203 (2021).(doi: [10.1103/PhysRevE.104.065203](https://doi.org/10.1103/PhysRevE.104.065203))
- ¹⁴W. L. Kruer, *The Physics of Laser Plasma Interactions* (Westview Press, Boulder, 2003).
- ¹⁵D. R. Nicholson, *Introduction to Plasma Theory* (John Wiley & Sons, New York, 1983).
- ¹⁶Z. J. Liu, B. Li, X. Y. Hu, J. Xiang, C. Y. Zheng, L. H. Cao, and L. Hao, Phys. Plasmas **23**, 022705 (2016).(doi: [10.1063/1.4941967](https://doi.org/10.1063/1.4941967))
- ¹⁷S. Skupsky, R. W. Short, T. Kessler, R. S. Craxton, S. Letzring, and J. M. Soures, J. Appl. Phys. **66**, 3456 (1989).(doi: [10.1063/1.344101](https://doi.org/10.1063/1.344101))
- ¹⁸B. J. Albright, L. Yin, and B. Afeyan, Phys. Rev. Lett. **113**, 045002 (2014).(doi: [10.1103/PhysRevLett.113.045002](https://doi.org/10.1103/PhysRevLett.113.045002))
- ¹⁹Z. J. Liu, C. Y. Zheng, L. H. Cao, B. Li, J. Xiang, and L. Hao, Phys. Plasmas **24**, 032701 (2017).(doi: [10.1063/1.4977910](https://doi.org/10.1063/1.4977910))
- ²⁰Z. J. Liu, Q. Wang, W. S. Zhang, B. Li, P. Li, W. G. Zheng, X. Li, J. W. Li, L. H. Cao, Y. K. Ding, and X. T. He, Phys. Plasmas **30**, 032703 (2023).(doi: [10.1063/5.0137403](https://doi.org/10.1063/5.0137403))
- ²¹Q. K. Liu, E. H. Zhang, W. S. Zhang, H. B. Cai, Y. Q. Gao, Q. Wang, and S. P. Zhu, Phys. Plasmas **29**, 102105 (2022).(doi: [10.1063/5.0105089](https://doi.org/10.1063/5.0105089))
- ²²M. F. Luo, S. Hüller, M. Chen, and Z. M. Sheng, Phys. Plasmas **29**, 032102 (2022).(doi: [10.1063/5.0078985](https://doi.org/10.1063/5.0078985))
- ²³M. F. Luo, S. Hüller, M. Chen, and Z. M. Sheng, Phys. Plasmas **29**, 072709 (2022).(doi: [10.1063/5.0096771](https://doi.org/10.1063/5.0096771))
- ²⁴Y. Zhao, L. L. Yu, J. Zheng, S. M. Weng, C. Ren, C. S. Liu, and Z. M. Sheng, Phys. Plasmas **22**, 052119 (2015).(doi: [10.1063/1.4921659](https://doi.org/10.1063/1.4921659))
- ²⁵Y. Zhao, S. M. Weng, M. Chen, J. Zheng, H. B. Zhuo, C. Ren, Z. M. Sheng, and J. Zhang, Phys. Plasmas **24**, 112102 (2017).(doi: [10.1063/1.5003420](https://doi.org/10.1063/1.5003420))
- ²⁶H. H. Ma, X. F. Li, S. M. Weng, Z. M. Sheng, and J. Zhang, Matter Radiat. Extremes **6**, 055902 (2021).(doi: [10.1063/5.0054653](https://doi.org/10.1063/5.0054653))
- ²⁷J. W. Bates, J. F. Myatt, J. G. Shaw, R. K. Follett, J. L. Weaver, R. H. Lehmburg, and S. P. Obenschain, Phys. Rev. E **97**, 061202(R) (2018).(doi: [10.1103/PhysRevE.97.061202](https://doi.org/10.1103/PhysRevE.97.061202))
- ²⁸H. Wen, R. K. Follett, A. V. Maximov, D. H. Froula, F. S. Tsung, and J. P. Palastro, Phys. Plasmas **28**, 042109 (2021).(doi: [10.1063/5.0036768](https://doi.org/10.1063/5.0036768))
- ²⁹L. Hao, J. Li, W. D. Liu, R. Yan, and C. Ren, Phys. Plasmas **23**, 042702 (2016). (doi: [10.1063/1.4945647](https://doi.org/10.1063/1.4945647))
- ³⁰O. Klimo, S. Weber, V. T. Tikhonchuk and J. Limpouch, Plasma Phys. Control. Fusion **52**, 055013 (2010). (doi: [10.1088/0741-3335/52/5/055013](https://doi.org/10.1088/0741-3335/52/5/055013))
- ³¹O. Klimo, V. T. Tikhonchuk, X. Ribeyre, G. Schurtz, C. Riconda, S. Weber, and J. Limpouch, Phys. Plasmas **18**, 082709 (2011).(doi: [10.1063/1.3625264](https://doi.org/10.1063/1.3625264))
- ³²Q. Wang, C. Y. Zheng, Z. J. Liu, L. H. Cao, Q. S. Feng, C. S. Liu and X. T. He, Plasma Phys. Control. Fusion **61**, 085017 (2019).(doi: [10.1088/1361-6587/ab2736](https://doi.org/10.1088/1361-6587/ab2736))
- ³³Q. Wang, C. Y. Zheng, Z. J. Liu, C. Z. Xiao, Q. S. Feng, H. C. Zhang and X. T. He, Plasma Phys. Control. Fusion **60**, 025016 (2018).(doi: [10.1088/1361-6587/aa98bb](https://doi.org/10.1088/1361-6587/aa98bb))
- ³⁴M. N. Rosenbluth, Phys. Rev. Lett. **29**, 565 (1972). (doi: [10.1103/PhysRevLett.29.565](https://doi.org/10.1103/PhysRevLett.29.565))
- ³⁵M. N. Rosenbluth, R. B. White, C. S. Liu, Phys. Rev. Lett. **31**, 1190 (1973).(doi: [10.1103/PhysRevLett.31.1190](https://doi.org/10.1103/PhysRevLett.31.1190))
- ³⁶S. Obenschain, N. Luhmann Jr, and P. Greiling, Phys. Rev. Lett. **36**, 1309 (1976). (doi: [10.1103/PhysRevLett.36.1309](https://doi.org/10.1103/PhysRevLett.36.1309))
- ³⁷C. L. Tang, J. Appl. Phys., **37**, 2945 (1966).(doi: [10.1063/1.1703144](https://doi.org/10.1063/1.1703144))